

1 **Supplementary Materials:**

2 **Hierarchical-Structured Microchip for Point-of-Care Immunoassays**
3 **with Dynamic Detection Range**

4 Lei Mou^{1,3}, Ruihua Dong¹, Binfeng Hu^{1,3}, Zulan Li⁴, Jiangjiang Zhang^{1,3}, Xingyu

5 Jiang^{*1,2,3}

6 ¹Beijing Engineering Research Center for BioNanotechnology and CAS Key Laboratory
7 for Biomedical Effects of Nanomaterials and Nanosafety, CAS Center for Excellence in
8 Nanoscience, National Center for NanoScience and Technology, No. 11 Zhongguancun
9 Beiyitiao, Beijing, 100190, P. R. China

10 ²Department of Biomedical Engineering, Southern University of Science and
11 Technology, No 1088, Xueyuan Rd., Xili, Nanshan District, Shenzhen, Guangdong,
12 518055, P. R. China

13 ³The University of Chinese Academy of Sciences, 19 A Yuquan Road, Shijingshan
14 District, Beijing, 100049, P. R. China

15 ⁴Reproduction Centre of the 306th Hospital of People's Liberation Army, No. 9, Anxiang
16 Beili, Chaoyang District, Beijing, 100101, P. R. China

17 E-mail address: jiang@sustech.edu.cn

18 **Supplementary Methods**

19 Stability of Patterned Antibodies on ES-PLC.

20

21 **Supplementary Figures and Tables**

22 Fig. S1 The portable device for microfluidic immunoassay chip.

23 Fig. S2 The chip and portable device for automatic microfluidic
24 immunoassay.

25 Fig. S3 Commonly used materials are used to prepare electrospun
26 membranes.

27 Fig. S4 Control of electrospinning time can get electrospun PLC film with
28 different thickness.

29 Fig. S5 Signal intensity analysis of these confocal microscopy images.

30 Fig. S6 Size distribution of the prepared AuNPs from TEM image result.

31 Fig. S7 DLS result of AuNPs before and after modifying with antibody and
32 enzyme.

33 Fig. S8 Condition optimization for detection of CRP.

34 Fig. S9 Condition optimization for detection of PCT using seven-channel
35 chip.

36 Fig. S10 Detection of IL-6 by the microfluidic immunoassay chip.

37 Fig. S11 Storage stability of patterned antibody on ES-PLC.

38 Table S1 The LOD of IL-6 PCT and CRP detection.

39 Table S2 Concentrations of biomarkers in the No. 2 reagent reservoir.

40 Table S3 The reproducibility of our microfluidic chip.

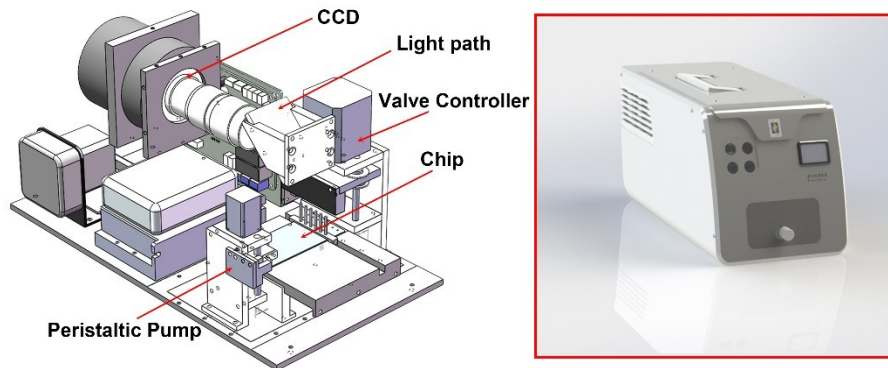
41 Table S4 Detection performance of our microfluidic chip.

42 **Supplementary Methods**

43 **Stability of Patterned Antibodies on ES-PLC.** To test the stability of the strip
44 over extended time of storage, we placed antibody-patterned strips at 37 °C in an
45 “accelerated stability studies”, where scientists believe that one day at this temperature is
46 equivalent to one month at 4 °C, before we carry out the assay. A set of chips were
47 assembled in the same way as described before. In order to verify the stability of
48 patterned antibodies on ES-PLC, we protected patterned antibodies with 5% sucrose
49 solution after blocking with BSA (**Fig. S11**). After incubating in 5% sucrose solution for
50 30 minutes, strip was dried. We assembled the strips into chips and placed them in a 37
51 °C oven. Every three chips were tested on day 0, day 2, day 4, day 6, day 8, and day 10
52 respectively. We added 20 ng/mL of PCT and 2000 pg/mL of IL-6 to the No. 2 reaction
53 reservoir. Signal attenuation was analyzed by the automatic device.

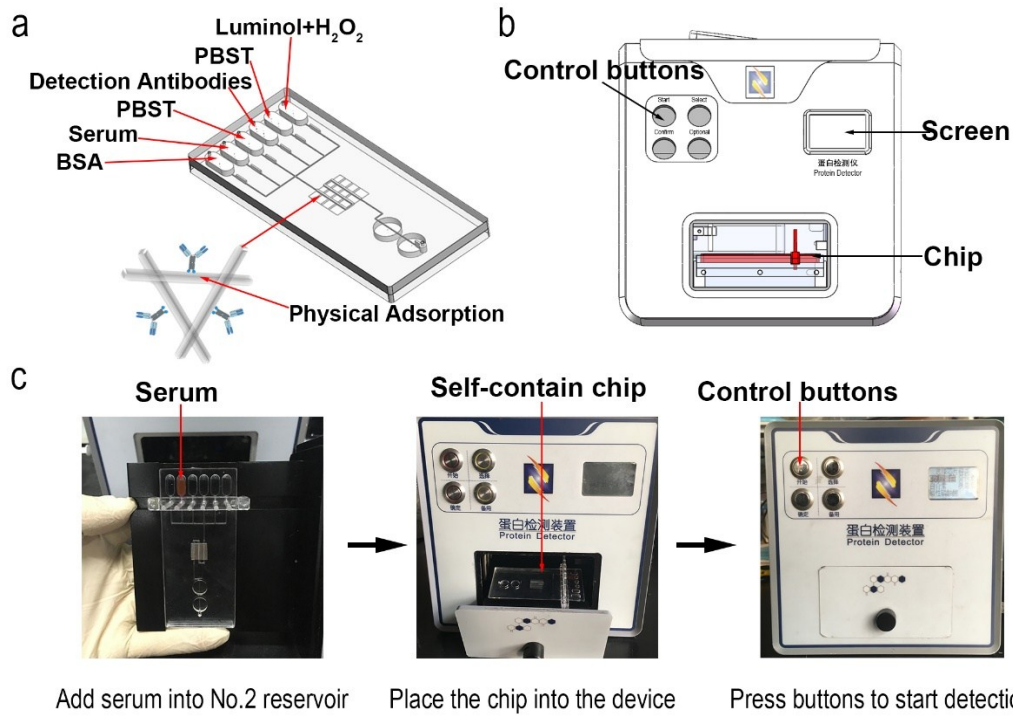
54 Experimental results indicate that the antibody-patterned strip could effectively
55 detect PCT and IL-6 after 10 days of baking. The red line shows the point where the PCT
56 signal is attenuated to 80% of its original value, while the blue line is IL-6 (**Fig. S11**).
57 These experiments indicate that these chips can be stably stored in refrigerator for ~6
58 months without significant attenuation of their signals.

59 Supplementary Figures and Tables



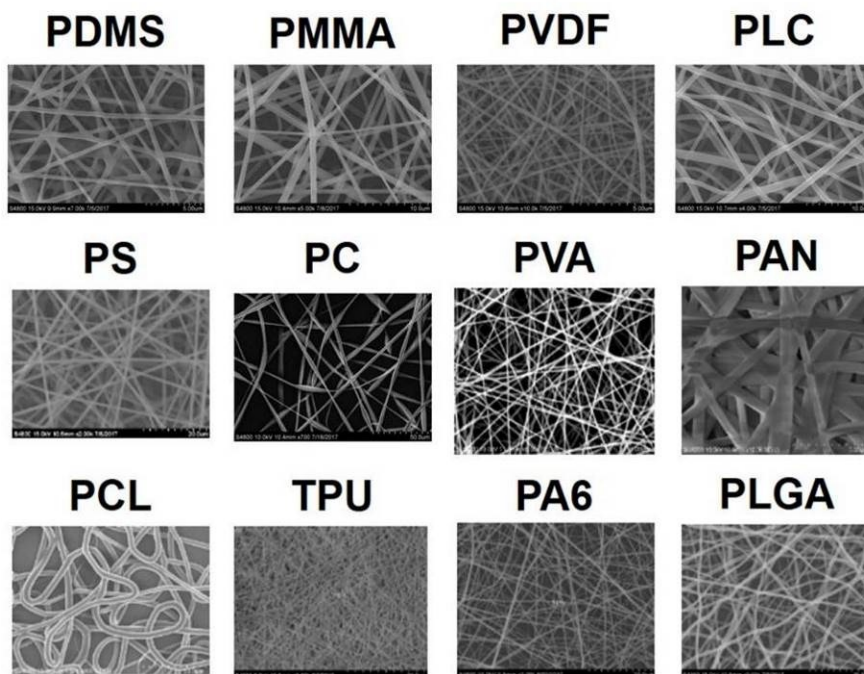
60

61 Fig. S1 The portable device for microfluidic immunoassay chip. The device mainly has
62 two functions: automatically drive the liquid to complete the whole assay; capture the
63 chemiluminescent signal to calculate the concentration of each biomarker. The valve
64 controller and peristaltic pump can drive fluids in accordance with program setting. The
65 chemiluminescent signal are guided by the light path and recorded by the CCD camera.



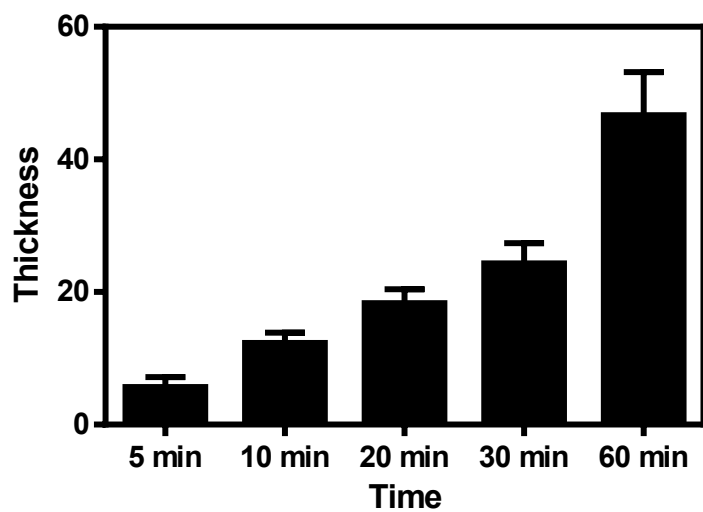
67 Add serum into No.2 reservoir Place the chip into the device Press buttons to start detection

68 Fig. S2 The chip and portable device for automatic microfluidic immunoassay. a) Self-
 69 contained chip with all required reagents for immunoassay. BSA, serum sample, PBST,
 70 detection antibodies, PBST and chemiluminescent reagents are added into reservoirs 1 to
 71 6, respectively. We use physical adsorption to allow the adsorption of antibodies onto the
 72 surface of tin-foil or ES-PLC, without any special pre-treatment. Physical adsorption is a
 73 commonly used antibody immobilization technique for immunoassays. b) Front-view of
 74 our portable device. When the chip is placed into the device, with a simple push of the
 75 control buttons can start the detection. The screen can provide real-time information to
 76 the users. c) Operation steps of our HMC-based autonomous DMI system. Step 1, add
 77 serum sample and reagents into reservoirs; Step 2, place the chip into the device; Step 3,
 78 press the buttons to start the detection.



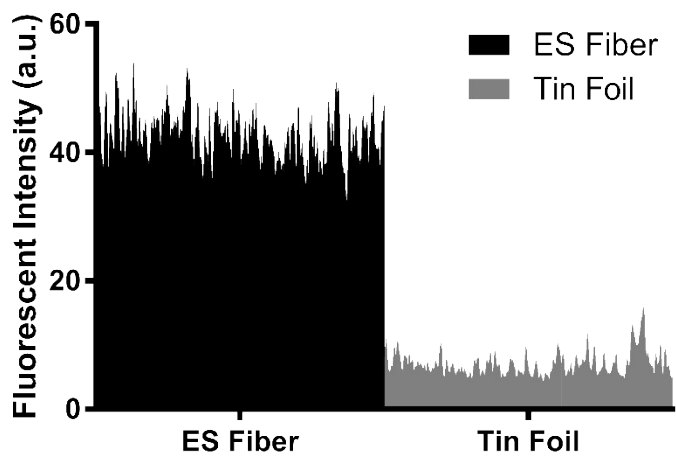
79

80 Fig. S3 Commonly used materials are used to prepare electrospun membranes.



81

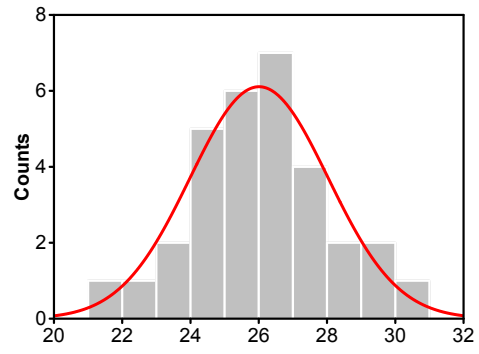
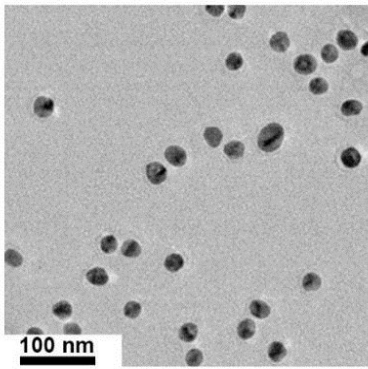
82 Fig. S4 Control of electrospinning time can get electrospun PLC film with different
83 thickness.



84

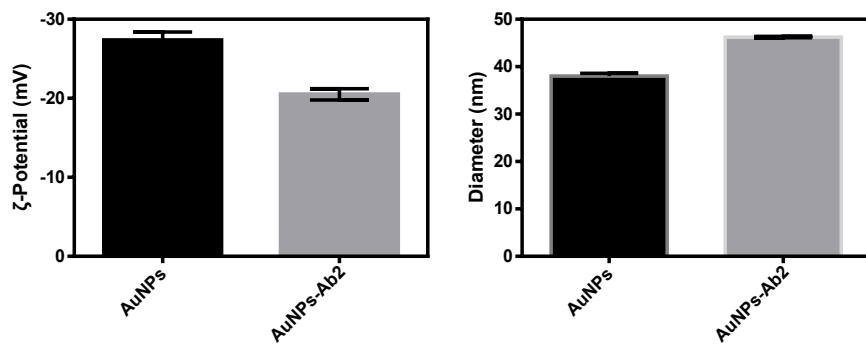
85 Fig. S5 Signal intensity analysis of these confocal microscopy images. Signal intensity

86 shows that its fluorescence signal increases nearly 7 times.



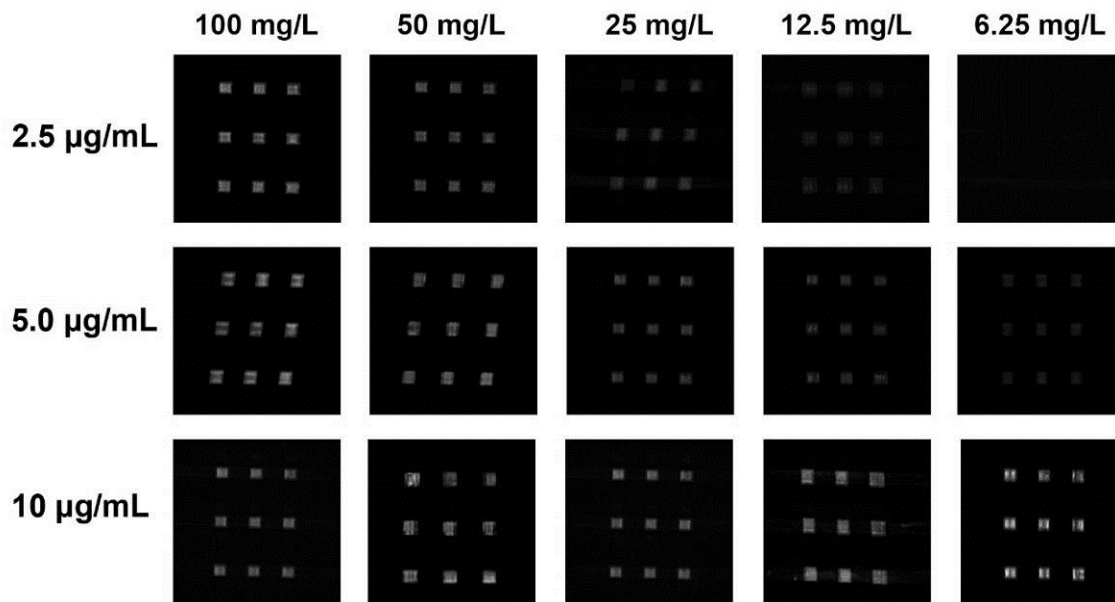
87

88 Fig. S6 Size distribution of the prepared AuNPs from TEM image result.



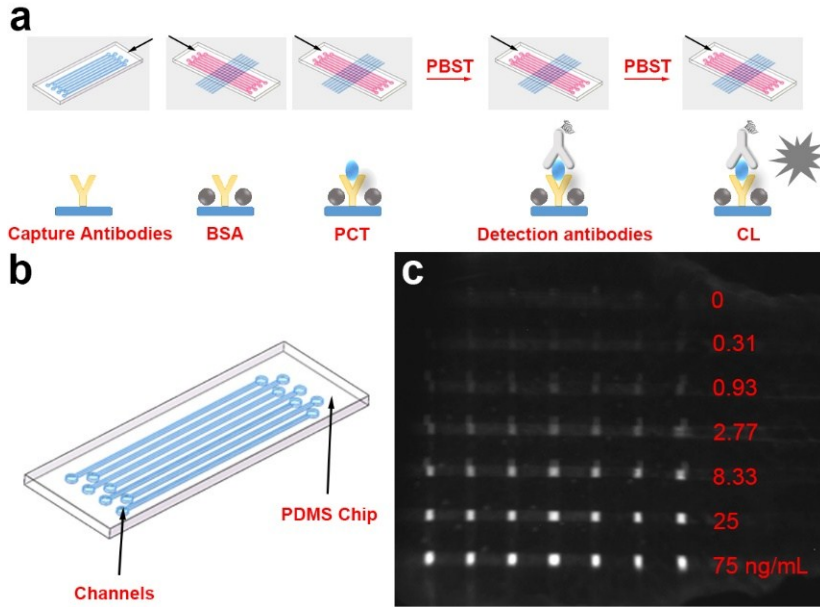
89

90 Fig. S7 DLS result of AuNPs before and after modifying with antibody and enzyme. ζ -
91 potential have a lightly decrease. Size distribution shows a slightly increase.



92

93 Fig. S8 Condition optimization for detection of CRP. CRP are detected by removing the
 94 ES-PLC film on the tin foil layer and lowering the concentration of patterned capture
 95 antibodies. Both higher and lower concentration of CRP can be detected with broad
 96 signal intensity when the concentration of capture antibodies is 5 $\mu\text{g/mL}$.



97

98 Fig. S9 The detection of PCT using seven-channel chip for detection condition

99 optimization. (a) Schematic illustration of the immunoassay procedure using seven-

100 channel chip for detection condition optimization. By placing two seven-channel chips on

101 the reaction substrate in a crisscross manner, 49 different reaction conditions can be

102 generated in one assay which can accelerate the progress of reaction condition

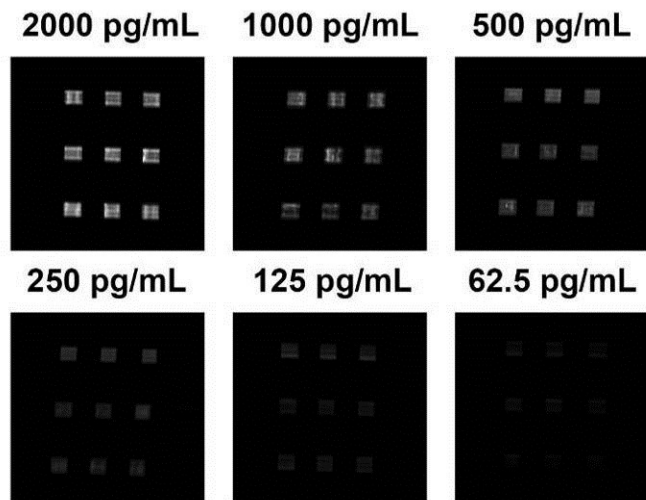
103 optimization. (b) Schematic illustration of the seven-channel chip. (c) When patterned the

104 PCT capture antibodies on the ES-PLC membrane with the concentration of 10 $\mu\text{g/mL}$,

105 the detection signal has a distinct gradient and the detection range meets clinical

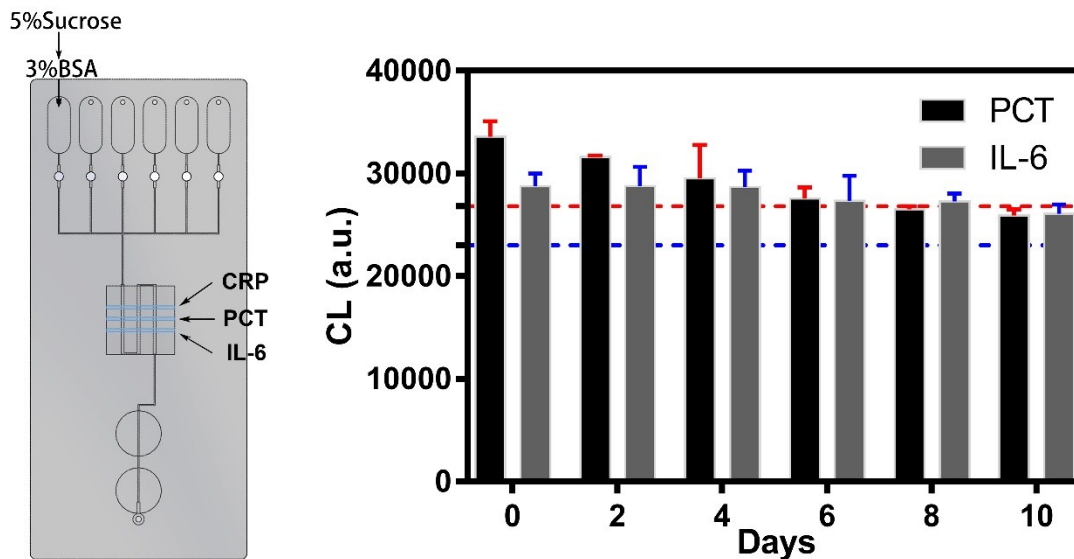
106 requirements.

107



108

109 Fig. S10 Detection of IL-6 by the microfluidic immunoassay chip. IL-6 is detected by
110 modifying the tin foil layer with electrospun microfibers to produce a porous three-
111 dimensional reaction layer and labeling detection antibody and enzyme onto AuNPs to
112 enhance the chemiluminescent signal. The detection range are from 2000 to 62.5 pg/mL
113 which can fit with the concentration in human serum sample. The concentration of
114 capture antibodies of IL-6 is 20 $\mu\text{g/mL}$.



115

116 Fig. S11 Storage stability of patterned antibody on ES-PLC, which is assessed by
 117 detecting standard PCT (20 ng/mL) and IL-6 (2000 pg/mL) samples inside microfluidic
 118 devices after being stored for various number of days at 37 °C. The red line shows the
 119 point where the PCT signal is attenuated to 80% of its original value, whereas the blue
 120 line is for an attenuation of the signal of IL-6 to 80% of its original value.

121 **Table S1** The LOD of IL-6 PCT and CRP detection.

	IL-6		PCT		CRP	
	CL	Calculated Concentration (pg/mL)	CL	Calculated Concentration (ng/mL)	CL	Calculated Concentration (µg/mL)
	(a.u.)		(a.u.)		(a.u.)	
Chip No. 1	623	40.21	1402	0.06	1100	1.78
Chip No. 2	592	38.06	1380	0.04	1299	1.85
Chip No. 3	550	35.13	1388	0.05	1162	1.80
Chip No. 4	504	31.92	1457	0.09	1179	1.81
Chip No. 5	661	42.87	1505	0.12	1201	1.81
Chip No. 6	680	44.19	1493	0.12	1225	1.82
Chip No. 7	548	34.99	1389	0.05	1135	1.79
Chip No. 8	522	33.17	1473	0.10	1099	1.78
Chip No. 9	631	40.77	1316	0.00	1024	1.76
Chip No. 10	604	38.89	1428	0.07	1198	1.81
Average		38.02		0.07		1.80
STD		3.91		0.04		0.02
Average+3STD		49.75		0.18		1.87

122 STD = standard deviation

123 The unit of absorbance is the arbitrary unit (a.u.).

124 **Table S2** Concentrations of biomarkers in the No. 2 reagent reservoir.

	CRP ($\mu\text{g/mL}$)	PCT (ng/mL)	IL-6 (pg/mL)
NO. 1	100	10	1000
NO. 2	0	0	1000
NO. 3	0	10	0
NO. 4	100	0	0

126 **Table S3** The reproducibility is tested with ten chips which contains the same
 127 concentration of biomarkers: IL-6 (1000 pg/mL) PCT (10 ng/mL) and CRP (10 µg/mL).

	IL-6		PCT		CRP	
	Calculated		Calculated		Calculated	
	CL	Concentration	CL	Concentration	CL	Concentration
		(pg/mL)		(ng/mL)		(µg/mL)
Chip No. 1	15749	1095	17010	9.85	7395	12.10
Chip No. 2	13784	958	17106	9.91	7235	11.60
Chip No. 3	16566	1152	20788	12.22	6665	9.98
Chip No. 4	14157	984	19879	11.65	6192	8.81
Chip No. 5	14558	1012	18237	10.62	6908	10.64
Chip No. 6	15806	1099	17392	10.09	7310	11.83
Chip No. 7	15304	1064	16611	9.60	6684	10.03
Chip No. 8	14272	992	15719	9.04	6777	10.28
Chip No. 9	13813	960	19704	11.54	6638	9.91
Chip No. 10	15878	1104	18110	10.54	7822	13.54
RSDs (%)		6.30		9.16		12.05

128 RSD: relative standard deviations

129 RSD= Sample standard deviation/ Mean value of the sample data set

130 The unit of absorbance is the arbitrary unit (a.u.).

131 **Table S4** Detection performance of our microfluidic chip.

Patient No.	IL-6 (pg/mL) (M±STD)	PCT (ng/mL) (M±STD)	CRP (µg/mL) (M±STD)
1	490±29	0.81±0.16	10.6±3.9
2	275±38	0.16±0.02	8.4±3.3
3	409±28	0.32±0.06	4.6±0.6
4	415±21	0.20±0.02	19.6±8.9
5	151±6	0.07±0.05	18.54±5.3
6	1064±81	9.74±0.53	104.2±35.4
7	387±18	1.86±0.38	3.6±0.3
8	422±20	5.72±0.40	12.7±1.6
9	460±17	9.30±0.26	3.3±0.1
10	626±40	3.15±0.24	17.9±7.2

132